Published in final edited form as:
Brain Struct Funct. 2013 September ; 218(5): 1293–1306. doi:10.1007/s00429-012-0458-6.

Zinc histochemistry reveals circuit refinement and distinguishes visual areas in the developing ferret cerebral cortex

Reem Khalil and
Department of Biology MR526, City College of New York, 160 Convent Avenue, New York, NY 10031, USA. Graduate Center of the City University of New York, 365 Fifth Avenue, New York, NY 10016, USA

Jonathan B. Levitt
Department of Biology MR526, City College of New York, 160 Convent Avenue, New York, NY 10031, USA. Graduate Center of the City University of New York, 365 Fifth Avenue, New York, NY 10016, USA

Jonathan B. Levitt: jlevitt@ccny.cuny.edu

Abstract

A critical question in brain development is whether different brain circuits mature concurrently or with different timescales. To characterize the anatomical and functional development of different visual cortical areas, one must be able to distinguish these areas. Here, we show that zinc histochemistry, which reveals a subset of glutamatergic processes, can be used to reliably distinguish visual areas in juvenile and adult ferret cerebral cortex, and that the postnatal decline in levels of synaptic zinc follows a broadly similar developmental trajectory in multiple areas of ferret visual cortex. Zinc staining in all areas examined (17, 18, 19, 21, and Suprasylvian) is greater in the 5-week-old than in the adult. Furthermore, there is less laminar variation in zinc staining in the 5-week-old visual cortex than in the adult. Despite differences in staining intensity, areal boundaries can be discerned in the juvenile as in the adult. By 6 weeks of age, we observe a significant decline in visual cortical synaptic zinc; this decline was most pronounced in layer IV of areas 17 and 18, with much less change in higher-order extrastriate areas during the important period in visual cortical development following eye opening. By 10 weeks of age, the laminar pattern of zinc staining in all visual areas is essentially adult like. The decline in synaptic zinc in the supra- and infragranular layers in all areas proceeds at the same rate, though the decline in layer IV does not. These results suggest that the timecourse of synaptic zinc decline is lamina specific, and further confirm and extend the notion that at least some aspects of cortical maturation follow a similar developmental timecourse in multiple areas. The postnatal decline in synaptic zinc we observe during the second postnatal month begins after eye opening, consistent with evidence that synaptic zinc is regulated by sensory experience.

Keywords

Visual cortex; Extrastriate; Synaptic zinc; Visual development

Correspondence to: Jonathan B. Levitt, jlevitt@ccny.cuny.edu.

Introduction

Interareal corticocortical projections are largely furnished by pyramidal neurons that utilize glutamate as their primary neurotransmitter. A subpopulation of glutamatergic neurons sequesters zinc into synaptic vesicles of their terminal boutons (Beaulieu et al. 1992; Martinez-Guijarro et al. 1991). This subpopulation could constitute an anatomically and functionally distinct subset of interareal projections, with distinct physiological properties. Furthermore, the cerebral cortex is characterized by a highly specific regional and laminar pattern of zinc staining (Dyck et al. 1993; Garrett et al. 1991, 1994). The supragranular and infragranular layers of cortical areas exhibit high zinc levels, while layer IV has the lowest levels. This pattern is especially obvious in primary sensory areas such as S1 and V1, and results because the thalamocortical recipient layer IV of primary sensory areas is nearly devoid of zinc-positive synapses (Casanovas-Aguilar et al. 1998; Garrett et al. 1992). Furthermore, zinc-rich corticocortical projections in the rat appear to be organized in a highly specific manner, forming two segregated systems, one arising from the supragranular layers and the other from the infragranular layers (Casanovas-Aguilar and Miro-Bernie 2002).

Synaptic zinc is known to be developmentally regulated in cat primary visual cortex (Dyck et al. 1993), rat and mouse forebrain (Garrett and Slomianka 1992; Valente et al. 2002) as well as mouse somatosensory cortex (Czupryn and Skangiel-Kramska 1997). Our aim in this study was to examine the change with age of the distribution of synaptic zinc in five visual cortical areas of the juvenile ferret from 5 to 10 weeks postnatal (as well as in adults) to establish the age at which synaptic zinc density is adult like. Ferrets (*Mustela putorius furo*) are ideal for use in developmental connectional studies because of their protracted postnatal period of brain development, and their relatively smooth cerebral cortex that facilitates access to all visual cortical areas. These ages were chosen to span the period just after eye opening, during which emergent visual responses undergo much of their refinement to the adult like state. We wished to determine if the change in zinc staining proceeds at the same rate in different visual areas. Of course accurate anatomical identification of these cortical areas is essential to the characterization of their anatomical and physiological development. In the course of these studies, we discovered that synaptic zinc histochemistry can be used to reliably distinguish visual areas in juvenile ferret visual cortex as early as 5 weeks postnatal. This is important since the myelination of juvenile ferret cortex is not complete until the end of the second postnatal month (Barnette et al. 2009); thus, the commonly used myelin stain to distinguish cortical areas in the adult is not a suitable anatomical marker of visual cortical areas in early postnatal development.

Here, we describe the developmental trajectory of zinc staining in five visual cortical areas of the ferret brain. We provide evidence for a decline in zinc staining in layer IV of several visual cortical areas in the period after eye opening; this change was most prominent in areas 17 and 18 (which unlike higher-order areas receive a prominent thalamic input from the lateral geniculate nucleus). We observed less of a decrease in staining in the supragranular and infragranular layers in all areas over this same period. Our measurements suggest that synaptic zinc levels in visual cortex are essentially adultlike by 6 weeks postnatal, and suggest that this aspect of cortical maturation follows a similar developmental timecourse in all visual cortical areas.

Materials and methods

Animal treatment

We studied twenty-four female ferrets (*Mustela putorius furo*) at five postnatal ages: 5 weeks ($n = 3$), 6 weeks ($n = 5$), 8 weeks ($n = 4$), 9 weeks ($n = 4$), and 10 weeks ($n = 3$), plus

adults ($n = 5$). Adult ferrets were sexually mature and at least 1 year old. Animals were obtained from Marshall Farms (North Rose, NY); kits were housed with the jill under a 12 h light/dark cycle. The ages of ferret kits were determined by their recorded birthdates. Some of these animals underwent anatomical injection experiments yielding data for a separate study; anatomical tracer injections were performed as described in Cantone et al. (2005). Histochemical markers are routinely used in conjunction with anatomical tracer injections, and typically do not affect tissue quality or staining. All procedures conformed to National Institutes of Health guidelines. Animals were lightly anesthetized with an intramuscular injection of ketamine (25 mg/kg) and xylazine (2 mg/kg), and then received an intraperitoneal injection of the zinc chelator sodium selenite (15 mg/kg). Following the injection, selenium salts travel to the brain and react with endogenous zinc, rendering precipitates that can be enhanced by silver development (Danscher 1982).

Tissue preparation

At 40–60 min after receiving the selenite injection, animals were euthanized with an overdose of sodium pentobarbital (100 mg/kg, i.p) and perfused transcardially with 0.9 % NaCl for 10 min, followed by 4 % paraformaldehyde for 20 min. A final 10 % sucrose in 4 % paraformaldehyde solution was used with a total fixation time of roughly 1 h. The brains were quickly removed from the skull, hemispheres were separated, and the posterior part of the brain was blocked and postfixed in 4 % paraformaldehyde in 0.1 M phosphate buffer (PB) for several hours. Blocks were then placed into a 30 % sucrose solution in 0.1 M PB. Once the brains were sunk, 40 μm thick sections were cut through visual cortex on a freezing, sliding microtome. The sections were separated into numbered series. For both juvenile and adult animals, one series was immediately mounted on egg white subbed slides, dried overnight at room temperature, and processed histochemically for synaptic zinc. For juveniles, another full series was processed for cytochrome oxidase using the modified protocol of Wong-Riley (1979): incubation for 2–8 h at 40 °C with 3 % sucrose, 0.015 % Cytochrome C, 0.015 % catalase and 0.02 % diaminobenzidine in 0.1 M PB, The remaining series for the adult animals was divided so that alternate sections were stained for myelin (Gallyas 1979) or cytochrome oxidase. Myelin-stained sections are not shown here.

Synaptic zinc histochemistry

Histochemical localization of synaptic zinc was revealed using a modification of the method described by Danscher (1982). This selenium-based histochemical method is specific for zinc in the brain that is localized to presynaptic vesicles of neurons that use zinc (Danscher et al. 1985; Frederickson 1989; Frederickson and Danscher 1988). The coincidence of the zinc distribution shown by silver amplification with that shown by specific zinc fluoroprobes confirms that the labeled metal in the vesicles is zinc (TSQ, zincquin: Frederickson et al. 1992); this TSQ fluorescent method produces bright fluorescence when complexed with zinc, but not when complexed with other transition metals such as iron or copper (Frederickson 2003). Briefly, slides were fixed in absolute alcohol for 15 min and allowed to dry at room temperature. Sections were then immersed briefly in a 1 % gelatin solution and allowed to dry at room temperature. The sections were then reacted in the dark in a freshly prepared silver developing solution containing the following: 60 ml of 30 % gum Arabic in dH_2O, 10 ml of 2.52 g citric acid plus 2.35 g sodium citrate in dH_2O at pH 4.0, 15 ml of 0.85 g hydroquinone in dH_2O, and 15 ml of 0.11 g silver lactate in dH_2O. Solutions were mixed in the order in which they were described. The sections were allowed to develop at room temperature in total darkness, and generally required 120–180 min for complete development. The development of the reaction was visually inspected every 30 min. Once the desired intensity was achieved, the reaction was terminated by rinsing the slides in warm water for 10 min to remove the gelatin coat and the outer silver deposit. Slides were allowed to dry at room temperature, and were then dehydrated in 100 % EtOH,

cleared in xylene, and cover slipped with Permount. Sections from three animals without previous selenite treatment (negative controls) underwent silver amplification but showed no staining; the lack of staining was independent of age.

Areal and laminar boundaries

The architecturally defined features of visual cortical areas in the adult ferret (Innocenti et al. 2002) were utilized to aid in the identification of different areas. The borders of cortical areas in the adult were determined by comparing the pattern of staining in myelin, cytochrome oxidase (CO), and synaptic zinc stain. Areal boundaries in the juveniles were similarly determined by comparison of the CO and synaptic zinc stain. Sections were examined and photographed with bright field illumination using a Nikon Eclipse Ti inverted scope at low power (4×) lens. Contrast and brightness of photomicrographs were enhanced in image processing software (Adobe Photoshop CS5, v.12) for display purposes, but were otherwise unaltered. Images used for optical density measurements were not altered in any way.

Densitometric analysis

To quantitatively assess the developmental change in zinc staining, we measured the optical density of selected zinc-stained sections in areas 17, 18, 19, 21, and Suprasylvian (Ssy) at 5, 6, 8, 9, and 10 weeks postnatal, and in the adult. This was accomplished by randomly choosing a cortical column 300–500 μm wide from photomicrographs spanning all cortical layers from the pial surface to the white matter. At least one sample column was chosen from each of at least three sections in each area, at each age. Column images were imported into ImageJ (NIH, v.1.44) and contrast inverted. Optical density profiles were generated from these images; each value in these profiles represents the average gray scale value at each depth across the width of the column. Because of variation in overall staining intensity across animals due to different reaction times, tissue stainability, and other variables, we use the relative density of synaptic zinc to make quantitative comparisons. To calculate relative zinc density, plot profile values were smoothed with a boxcar average of every successive 20 pixels (1 pixel = 2.5 μm) in depth, and normalized to maximum intensity for each sample. We also used a second normalization whereby density values were produced by dividing each value by the mean white matter value for each section. White matter optical density values were obtained from sample cortical columns (300–500 μm wide) that included the underlying white matter (approximately 150 μm below layer 6) in areas 17, 18, and Ssy. The white matter values obtained at each age below each area were similar, and were averaged together. We then calculated the mean minimum pixel value in the lightly stained region of layers IV and VI, and the mean maximum pixel value in layer V. Mean values were determined in the depth range encompassing the minimum or maximum value by ±5 pixels. The mean pixel intensity of the supragranular and infragranular layers was also calculated. The limits of layer IV, supragranular, and infragranular layers in the contrast-inverted images were judged by comparison with the original photomicrographs as well as the adjacent CO section. This allowed us to be confident of the identity of each layer examined, and precluded the possibility of intruding on adjacent layers.

All statistical analyses were performed in MATLAB (The Mathworks, Natick, MA). We used the Kruskal–Wallis test to assess statistical differences in mean optical density values among age groups and areas with a significance level of $p < 0.05$. Post hoc pair-wise comparisons between ages (in each area) and areas (at each age) were then computed using a Bonferroni correction.

Results

Synaptic zinc staining distinguishes visual cortical areas in adult and juvenile ferret brain

Visual cortical areas in the adult ferret are readily distinguishable with the aid of several histochemical markers, such as those for myelin and cytochrome oxidase (CO). The cytoarchitecture and myelination patterns of different visual areas in the adult ferret cortex have been well characterized (Innocenti et al. 2002; Cantone et al. 2005). Here, we demonstrate that synaptic zinc staining similarly differs among visual cortical areas, even in the juvenile cortex.

Areal boundaries and laminar features of zinc staining in adult and juvenile ferret visual cortex

Adult and 5-week-old

Areas 17 and 18: The distribution of synaptic zinc staining in the adult ferret visual cortex is illustrated in a representative semi-tangential section in Fig. 1a. The arrows mark areal boundaries. In general, intense synaptic zinc staining is observed in layers I, II, III, and V (though we note that layer 1 stains more intensely in areas 17 and 18 than in areas 19, 21, and Ssy); layer VI is only moderately stained, while layer IV is nearly devoid of zinc. The adjacent section stained for cytochrome oxidase (CO) (Fig. 1b) reveals similar locations of areal boundaries and illustrates the reciprocal nature of CO and synaptic zinc in layer IV; in areas 17 and 18 regions of low zinc staining generally correspond to those of high CO staining. A high power view of the laminar features of zinc staining in the adult is illustrated in Fig. 2a. Representative photomicrographs of columns from pia to white matter were taken from each visual cortical area. Area 17 is to the left with successively more rostral areas to the right. The cortical layers are indicated by the roman numerals. Primary visual cortex (area 17) and area 18 are unique in that layer IV stain very lightly (Figs. 1a, 2a). The lack of zinc staining in layer IV of area 17 contrasts with the intensely labeled layer IV band found in CO-stained material (Fig. 1b); the darkly stained layer IV in area 17 maintains a sharp border with layers III and V. The high power columnar photomicrographs of adjacent sections better illustrate the laminar CO reactivity pattern in each area in Fig. 2b.

Synaptic zinc staining in area 18 is qualitatively similar to area 17 with subtle laminar differences. Layers IV and V of area 18 stain even lighter than in area 17 (Figs. 1a, 2a). Layer VI is characterized by its bipartite staining with a moderately stained sublamina just below layer V, and a thin darkly stained sublamina just above the white matter. This is more clearly seen in the low power view in Fig. 1a. In CO preparations (Figs. 1b, 2b), the intense layer IV band characteristic of primary visual cortex is maintained in area 18 with a slight decrease in intensity. Moreover, the upper boundary of this band blurs with layer III, but maintains a sharp border with layer V (Fig. 2b).

The distribution of synaptic zinc in a semi-tangential section at 5 weeks of age is depicted in Fig. 1c. The most striking difference in zinc staining between the 5-week-old and the adult is that the overall staining intensity is greater in the juvenile. Similar to the adult, the supragranular layers, and layer V of areas 17 and 18 stain very intensely, while layer VI is of moderate intensity. Layer I in all areas of the 5-week-old stains very intensely. Also similar to the adult is the subtle decrease in zinc intensity in area 18 relative to area 17 (Figs. 1c, 2c). Unlike the adult, however, layer IV of areas 17 and 18 is of moderate intensity. Similar to the adult, the intense CO band occupying layer IV characteristic of area 17 is maintained in area 18 with a slight decrease in intensity (Fig. 2d). Moreover, the upper boundary of this band blurs with layer III, but maintains a sharp border with layer V (Fig. 2d).

Area 19: The distribution of synaptic zinc in adult area 19 is different than in areas 17 and 18 in that there is less laminar variation (Figs. 1a, 2a), as well as a thinner and moderately stained layer IV that fills in. Layers IV and VI of area 19 are of similar intensity, while the supragranular layers and layer V stain intensely. In the complementary CO section (Figs. 1b, 2b), there is little CO staining in area 19, with a weak and inconsistent CO band in layers III and IV. Area 19 in the 5-week-old also has less laminar variation in zinc staining, but greater staining intensity than area 19 of the adult (Fig. 1c). As in the adult, area 19 of the 5-week-old is characterized by very low CO reactivity (Figs. 1d, 2d).

Area 21: Area 21 has a qualitatively similar synaptic zinc distribution as area 19 (Figs. 1a, 2a), with a very subtle increase in intensity in layer IV. However, the bottom of layer VI stains more intensely in area 21 than in area 19. In CO-stained material (Figs. 1b, 2b), area 21 is characterized by the reappearance of the layer III/IV band present in area 18. Area 21 of the 5-week-old shows a slight increase in laminar variation with a thinner layer IV that is comparable in zinc intensity to layer VI (Fig. 2c). In CO-stained material (Figs. 1d, 2d), area 21 is characterized by the reappearance of the layer III/IV band present in area 18.

Suprasylvian cortex (Ssy): Ssy lies immediately rostral and ventral to area 21, and lies along the posterior bank of the Suprasylvian sulcus (SsyS). In zinc-stained sections, Ssy is characterized by a pale and thin layer IV, and pale layer VI. Layer V stains intensely and the supragranular layers are of variable intensity (Fig. 1a). In CO-stained material, it can be distinguished from adjoining areas mainly in the supragranular layers (Fig. 1b). The supragranular layers are more intensely stained than the adjoining caudal posterior parietal (PPc) and lateral temporal visual areas.

The laminar variation in zinc staining characteristic of Ssy in the 5-week-old is comparable to that in area 21, with a slight decrease in zinc intensity in layer VI (Figs. 1c, 2c). The dark CO band reappears in layer IV of area 21 and Ssy. However, layer VI of Ssy shows more CO reactivity relative to that in area 21 (Fig. 2d). Although there is less laminar variation across areas and an overall greater staining intensity in the 5-week-old than in the adult, areal boundaries in the 5-week-old correlate well with boundaries observed in the adult (Fig. 1c).

As further confirmation of the observed staining patterns, Fig. 1e–h shows adjacent semi-tangential sections of the thalamus in the adult and 5-week-old stained for zinc or CO. The lack of zinc staining in the lateral geniculate nucleus of the thalamus, indicated by the arrow, is consistent with previous reports (Dyck et al. 1993; Valente et al. 2002). Taken together, the lack of staining in the LGN and white matter, and the observed areal and laminar differentiation of zinc staining, suggests that the dark zinc staining in visual cortex of younger animals is genuine.

Nine-week-old

Areas 17 and 18: The zinc staining and CO reactivity in the visual cortex of the 9-week-old are shown in Fig. 3a and b respectively. The semi-tangential zinc and CO sections in Fig. 3a were taken at a similar cortical depth to the representative sections from the 5-week-old and adult. By 9 weeks of age, the areal and laminar pattern of synaptic zinc across areas is nearly identical to that found in the adult. Columnar photomicrographs taken from a section in a 9-week-old stained for synaptic zinc are shown in Fig. 3c. Similar to the adult (and unlike the 5-week-old), layer IV of areas 17 and 18 in the 9-week-old is only lightly stained. Further, layer IV of area 18 is slightly paler than layer IV of area 17. Areas 17 and 18 show stereotypical high intensity staining in the supragranular layers as well as in layer V, layer VI is of moderate intensity, while layer IV is of very low intensity.

Area 19: Similar to the adult, the distribution of synaptic zinc in area 19 of the 9-week-old is clearly different than in areas 17 and 18. There is less laminar variation (Fig. 3a, c) in area 19, and the most obvious difference is the thinner and moderately stained layer IV that fills in. In the complementary CO section (Fig. 3b, d), there is little CO staining in area 19, with a weak and inconsistent CO band in layers III and IV.

Area 21: The subtle laminar variation in zinc staining found in area 21 of the adult is also seen in area 21 of the 9-week-old (Fig. 3a, c). The complementary adjacent CO section shown in Fig. 3b similarly reveals a staining pattern shared between the 9-week-old and adult. The laminar pattern of CO reactivity unique to each area shared in the 9-week-old is better illustrated in Fig. 3d.

Suprasylvian cortex (Ssy): Both the laminar distribution of zinc staining and pattern of CO reactivity observed in the adult are also seen in the 9-week-old. The laminar variation in zinc staining characteristic of Ssy in the 9-week-old is comparable to that in area 21, with a slight decrease in zinc intensity in layer IV (Fig. 3a, c). The dark CO band reappears in layer IV of area 21 and Ssy. However, layer VI of Ssy shows more CO reactivity relative to that in area 21 (Fig. 3d).

At all postnatal ages, areal transitions in zinc staining correlate well with those seen in CO staining. Furthermore, areal transitions seen in zinc staining and CO staining in the juvenile are consistent with those observed in the adult.

Quantitative changes in synaptic zinc density during development

We quantitatively assessed the distribution of synaptic zinc in all visual cortical areas at several postnatal ages; comparisons between the 5-week-old and adult revealed a significant decline in zinc density in layer IV. Optical density values were normalized to the maximum intensity value in that section. Plots of normalized optical density values were then constructed as a function of cortical depth. Each value in these profiles represents the average gray scale value at successive cortical depths. Columnar photomicrographs of representative adult zinc-stained sections and their complementary normalized optical density plot profiles are shown in Fig. 4a. The most striking feature is the trough in the plot profile of areas 17 and 18 that corresponds to the low zinc density in layer IV. The filled-in ovals represent the mean minimum pixel intensity value. This significant drop in zinc density in layer IV of areas 17 and 18 is less obvious in areas 19, 21, and Ssy, and is demonstrated by the subtle dip within layer IV. Typically, the supragranular layers and layer V of areas 17 and 18 stain more intensely than layer VI.

In contrast, we find a significantly different pattern in the 5-week-old (Fig. 4b). Optical density measures reveal more intense zinc staining in layer IV of areas 17 and 18 (indicated by the subtle dip in the plot profile) relative to that found in the adult. However, zinc staining density in layer IV of areas 19, 21, and Ssy is only slightly greater in the juvenile relative to that in the adult. Both the supragranular and infragranular layers appear to have greater synaptic zinc density in the 5-week-old relative to the adult.

The greater dip in relative zinc staining density in adult layer IV might reflect different changes with age in absolute zinc staining in different cortical layers. We therefore compared the synaptic zinc optical density in layer IV of each area to the mean values in the supragranular and in-fragranular layers. We calculated ratios of zinc optical density in layer IV to the mean of that in both supra- and infragranular layers, and plotted values as a function of age (Fig. 5). The mean ratio of optical density in layer IV compared to the upper layers (LIV/supra) in all areas of the 5-week-old was 0.95, indicating nearly equal zinc staining in layers II/III and IV of these areas (Fig. 5a). By 6 weeks of age, the mean ratios in

areas 17 and 18 (dashed and dotted lines, respectively) decrease markedly to 0.62 (p <0.05). However, there is a modest decline from 10 weeks until adulthood, suggesting a more protracted developmental process. The LIV/supra ratios in areas 19, 21, and Ssy (long dashed and dotted, short dashed, and solid lines, respectively) show a less prominent decline from 0.95 to 0.90 from 5 to 6 weeks of age. From 6 weeks until adulthood, the ratios in all areas remained essentially unchanged with no significant differences among ages.

Similar to LIV/Supra ratios, ratios of optical density between those in layer IV and infragranular layers (LIV/ Infra) are initially high (mean 0.98) in all areas of the 5-week-old (Fig. 5b). By 6 weeks of age, the ratios in areas 17 and 18 (dashed and dotted lines, respectively) show a marked decrease to 0.66 (p <0.05). From 6 to 10 weeks of age LIV/ infra ratios in areas 17 and 18 are relatively stable, with a gradual decline from 10 weeks until adulthood. Areas 19, 21 and Ssy (long dashed and dotted, short dashed, and solid lines, respectively) show a subtle decrease to 0.96 from 5 to 6 weeks of age, with ratios remaining unchanged thereafter, with no significant differences among ages. From 6 weeks of age, the LIV/infra ratios in areas 17 and 18 remain significantly different than the LIV/infra ratios in areas 19, 21, and Ssy (p <0.05).

We further separately quantified the relative mean optical density of synaptic zinc in layer IV, supra- and infragranular layers to reveal whether the postnatal declines in (LIV/supra) and (LIV/infra) ratios were due to a decrease in optical density in specific layers. The decline in the (LIV/supra) and the (LIV/infra) ratios may be due to a decrease in zinc density in layer IV and an increase in zinc density in the supra- or infragranular layers. However, our findings show that the zinc density decreases with age in all layers, though most in layer IV.

Unlike the values obtained previously from the LIV/ Supra and LIV/Infra ratios whereby each normalized plot profile value was divided by the mean value in the supra-granular or infragranular layers, the relative mean optical density in LIV, supragranular, and infragranular layers is simply normalized to the highest pixel value in each sample. The mean relative optical density of synaptic zinc in layer IV of all visual areas is plotted as a function of age in Fig. 6a. Typically, the mean relative layer IV optical density in all areas of the 5-week-old was high (94 %). By 6 weeks of age, mean relative optical density in layer IV of areas 17 and 18 (dashed and dotted lines, respectively) decreased to 60 % (p <0.05). From 10 weeks until adulthood we observe a gradual decrease in mean relative optical density in layer IV of areas 17 and 18, suggesting a longer maturation phase. Areas 19, 21, and Ssy (long dashed and dotted, short dashed, and solid lines, respectively) showed a less prominent yet statistically significant (p <0.05) drop in mean relative optical density in layer IV from 5 to 6 weeks, as well as a slow decrease from six weeks until adulthood. Therefore, it appears that zinc staining in layer IV of areas 17 and 18 decreases more than in layer IV of areas 19, 21, and Ssy. From 6 weeks until adulthood, mean relative optical density in layer IV remains unchanged in areas 19, 21, and Ssy. At all ages examined, the mean relative optical densities in layer IV of areas 17 and 18 are significantly lower (p <0.05) than in layer IV of areas 19, 21, and Ssy.

The relative optical density in the supragranular layers initially averages 97 % in all areas of the 5-week-old (Fig. 6b). All areas show a subtle insignificant decrease in relative optical density from 5 to 6 weeks of age (to a value of 94 %). From 6 weeks to adulthood, relative supragranular optical density values appear essentially unchanged. Similarly, relative zinc optical densities in the infragranular layers in all areas of the 5-week-old are high (95 %) (Fig. 6c). By 6 weeks of age, areas 17 and 18 exhibit a similarly modest, yet significant decrease in relative optical density in their infragranular layers (p <0.05), while areas 19, 21, and Ssy show a subtle and insignificant decrease in relative optical density in their

infragranular layers. It therefore appears that the developmental decline in the LIV/supra and LIV/infra ratios is largely due to the decrease in the relative optical density of zinc in layer IV, with a minor contribution from the decline in relative optical density of zinc in the supragranular and infragranular layers.

We sought to confirm the major decline in relative zinc density in layer IV as well as the minor decline in the supra- and infragranular layers of all areas by normalizing optical density values of synaptic zinc to the mean white matter (WM) value in each sample. The mean white matter value serves as a baseline measure against which gray matter values could be compared. The relative optical density values reflect the proportion of zinc density relative to the maximum pixel value in each section. Maximum pixel intensity may be the same for some ages; revealing the WM-normalized values with age, thus seems more informative as it allows us to unequivocally assert that overall staining intensity is greater in the juvenile, and that the decline in zinc density in layer IV is most pronounced in areas 17 and 18. We therefore calculated WM-normalized optical density values by dividing each plot profile value by mean white matter (WM) value in each section. We did not observe a developmental change in the white matter values. In fact, white matter values were very similar across all examined ages, except at 8 weeks of age. This is why we observe a dip in optical density in the gray matter from 6 to 8 weeks of age. For some reason, the white matter in these cases was darker than the white matter at other ages (even though some structures like the LGN remained unstained as in other cases). Higher white matter values yielded smaller ratios causing the observed dip. Figure 6d shows the WM-normalized optical density values in layer IV as a function of age. Like the relative optical density values in Fig. 6a, the WM-normalized values in layer IV of all areas in the 5-week-old were relatively high (mean 6.4). By 6 weeks of age, WM-normalized mean optical density values in areas 17 and 18 (dashed and dotted lines, respectively) drop significantly to 2.3, while areas 19, 21, and Ssy (long dashed and dotted, short dashed, and solid lines, respectively) showed a less prominent, yet still, significant drop in mean optical density in layer IV (mean 3.4).

The WM-normalized mean optical density value in the supragranular layers of all areas of the 5-week-old is 6.7 (Fig. 6e). All areas show a similarly significant decrease in optical density at 6 weeks of age (mean 3.8). Similarly, Fig. 6f shows that the WM-normalized optical density values in the infragranular layers in all areas of the 5-week-old are high (mean 6.5), but undergo a significant decline by 6 weeks of age (mean 3.6). These data corroborate our previous results, and show that the rate and magnitude of decline in the optical density of both the infragranular and supragranular layers are comparable across all five areas.

Discussion

We have shown that synaptic zinc staining can be used to distinguish visual areas in the adult and developing ferret cerebral cortex. Although zinc staining in the juvenile is darker with less obvious laminar variation than adults, the laminar pattern is discernible; areal boundaries were consistently identifiable and correlated well with boundaries found in the adult. In both juvenile and adult ferret, laminar staining patterns differ among areas; this differs among species. For example, our results show that layer I is dark in all areas in young animals, and darker in areas 17 and 18 than in 19, 21, and Ssy in the adult. Layer I in adult cat area 17 is dark (and distinguishable from layer II), but is dark and indistinguishable from layer II in areas 18 and 19 (Dyck et al. 1993). Brown and Dyck (2004) showed that layer I stains intensely in multiple cortical areas of the mouse forebrain, but layer Ia is zinc-poor in rat S1 (Land and Shamalla-Hannah 2002) and macaque TEO (Ichinohe et al. 2010). Therefore, it appears that regional and laminar differences are species specific.

To our knowledge, this is the first study to simultaneously investigate the developmental trajectory of zinc circuits in multiple visual cortical areas. We have shown that synaptic zinc staining in all layers of all five areas studied declines dramatically and on a broadly similar timecourse. By 6 weeks of age, we observe a significant decline in visual cortical synaptic zinc; this decline was most pronounced in layer IV of areas 17 and 18, with much less change in higher-order extrastriate areas during the important period in visual cortical development following eye opening. Synaptic zinc is a calcium- and activity-dependent neuromodulator implicated in synaptic function and plasticity (for review see Nakashima and Dyck 2009), and thus likely to play a key role in experience-dependent reorganization of visual circuits.

Previous studies have demonstrated the use of zinc histochemistry in distinguishing cortical areas in adult mouse (Garrett et al. 1991, 1994; Brown and Dyck 2004), developing and adult rat (Pérez-Clausell 1996; Valente et al. 2002), and developing and adult cat (Dyck et al. 1993). We demonstrate here that zinc histochemistry similarly distinguishes cortical areas in the developing ferret visual cortex. While visual cortical areas in the adult ferret cortex may easily be distinguished based on cyto-, chemo- and myeloarchitecture, it is more difficult to do so in young ferrets as the myelination of visual cortical areas is not complete until the end of the second postnatal month (Barnette et al. 2009). Another criterion used to identify cortical areas is the connectional pattern unique to each area (Kaas 2002). Synaptic zinc histochemistry can be interpreted as another indicator of an area's connectional pattern. This is so because the laminar zinc distribution unique to each area reflects a particular set of afferents.

Zinc histochemistry, like other histochemical markers, at some areal boundaries reveals transition zones and not necessarily sharp boundaries, but one can still distinguish areas reliably. Furthermore, areal boundaries we observe are broadly consistent with previous studies (Homman-Ludiye et al. 2010; Innocenti et al. 2002). Zinc histochemistry may prove useful in other cortical areas or sensory systems, although with some limitations. Many studies have reported that levels of synaptic zinc can be rapidly and dynamically regulated in conditions of sensory deprivation (Brown and Dyck 2002; Dyck and Chaudhuri 2003), so use of zinc as an areal marker necessarily assumes normal visual experience.

What circuits are being revealed?

In the adult ferret, layer IV of areas 17 and 18 receives a substantial LGN input, while areas 19, 21, and Ssy do not. The relative lack of zinc staining in layer IV of adult areas 17 and 18 presumably reflects the lack of zinc in geniculocortical terminals (Casanovas-Aguilar et al. 1998; Brown and Dyck 2004). The intense zinc staining in layer IV of juvenile ferret areas 17 and 18 suggests a developmental loss of zinc from thalamocortical afferents; this is consistent with Ichinohe et al.'s (2006) report of transient presence of zinc in thalamic afferents to rat barrel cortex. Layer IV of areas 19, 21 and Ssy is instead largely occupied by feed forward corticocortical terminals. Corticocortical terminals have been shown to sequester zinc (Garrett et al. 1992; Casanovas-Aguilar et al. 1995, 1998; Casanovas-Aguilar and Miro-Bernie 2002; Brown and Dyck 2004). Consistent with this finding, the relatively high zinc staining we observe in layer IV of these areas suggests that corticocortical feed forward input terminals are rich in synaptic zinc (though we do note that layer IV in area 18 appeared to stain less intensely for zinc than area 17). Our results suggest that there is either a decrease in the number of thalamocortical terminals in layer IV through postnatal development, or a decrease in the proportion of those terminals containing synaptic zinc, or a decrease in the amount of zinc in each terminal.

Alternatively, the dramatic decline we observe in synaptic zinc in layer IV of areas 17 and 18 could also be a consequence of the loss of early functional inputs from subplate neurons.

Subplate neurons are a transient neuronal cell population that is integral in the functional development of thalamocortical connections and ocular dominance column formation (Ghosh and Shatz 1992; Kanold et al. 2003). They provide the first postsynaptic targets for afferent thalamocortical axons (McConnell et al. 1989; Molnar et al. 1998), and project into the cortical plate (Finney et al. 1998; Friauf et al. 1990). This projection is mainly glutamatergic (Finney et al. 1998). We speculate that the synaptic zinc staining we observe in layer IV of areas 17 and 18 reflects transient input from subplate neurons that sequester high levels of zinc at their terminals; these could later be replaced by thalamic axons that sequester very little zinc at their terminals.

Using intracerebral injections of sodium selenite to retrogradely label zinc-positive neurons, Casanovas-Aguilar et al. (1995) examined the origin of zinc-positive pathways in rat visual cortex and revealed ipsilateral as well as callosal label. This study showed that labeled neurons were present in layers II–III and VI. Similarly, Brown and Dyck (2005b) showed that zinc-positive projections arise exclusively from within the cortex and reciprocally interconnect the mouse barrel cortex with other cortical and limbic regions. Their results demonstrated that the majority of zinc-positive projections to the barrel cortex arose from ipsilateral and callosal neurons, in the superficial and deep layers. Several lines of evidence suggest that a subset of intrinsic connections within an area is also zinc positive. Casanovas-Aguilar et al. (1998) mapped the zinc-positive afferents in rat neocortex by tracing zinc-positive projections to the visual cortex with intracerebral selenite injections. Selenite injections in several visual cortical areas (Oc1, Oc2M, and Oc2L) yielded a substantial number of zinc-positive neurons within each area. Brown and Dyck (2005b) similarly used selenite injections to reveal intrinsic connections in the superficial and deep layers of rat somatosensory cortex. Further evidence that zinc-positive neurons constitute a subset of intrinsic connections comes from Ichinohe et al. (2010). Using focal injections of sodium selenite into multiple visual cortical areas of the macaque ventral stream, they reported zinc-positive labeled intrinsic connections with an area-dependent laminar distribution.

Zinc-rich corticocortical projections appear to be a major component in the general system of feedforward and feedback circuits. Retrograde tracing of zinc-positive neurons was also utilized by Casanovas-Aguilar and Miro-Bernie (2002). They examined the regional and laminar distribution of zinc-positive neurons in the rat visual cortex. Their findings revealed a laminar distribution of zinc-positive neurons typically observed in feedforward and feedback projections between multiple visual cortical areas. Zinc-positive projections from Oc1 to Oc2L (feed-forward projections) were numerous and arose preferentially from supragranular layers, whereas feedback projection neurons (from Oc2M to Oc2L, or from Oc2L to Oc1) were more abundant in the infragranular layers. Ichinohe et al. (2010) further reported zinc-positive neurons in several feedback pathways after selenite injections in areas V1, V4, and TEO of macaque visual cortex. Surprisingly, unlike the results obtained by Casanovas-Aguilar and Miro-Bernie (2002) showing that zinc-positive neurons were found in both the feedforward and feedback pathways in rat visual cortex, Ichinohe et al. (2010) report that feedforward pathways are zinc negative in macaque. Feedback projections have been shown to originate mainly from the infragranular layers and terminate densely in layer I (Rockland and Pandya 1979). This is consistent with the pattern of zinc staining we observe in the adult ferret visual cortex. Zinc staining in layer I of areas 17 and 18 is consistently more intense than in layer I of areas 19, 21, and Ssy. This presumably reflects corticocortical feedback projections to areas 17 and 18 from higher visual areas. Therefore, it seems that zinc-positive inputs are a subclass of callosal, intra- and interareal connections; the staining we observe reflects the axon terminals of these cells.

Comparison with other developmental events and other species

The ages examined in this study (5–10 weeks postnatal) were chosen to span the period just after eye opening (around P32 in ferret), during which emergent visual responses undergo much of their refinement to the adultlike state. These ages are approximately equivalent to: P12–P24 in a mouse, P15–P30 in a rat, P18–P56 in a cat, and E154–P65 in macaque monkey (extrapolated from Clancy et al. 2001). For example, mice typically open their eyes around P12, rats around P15, cats around P7, and macaque monkeys are born with their eyes open. The ferret brain is perhaps more immature at birth than cats and monkeys; for example, the differentiation and neurogenesis of layer IV of primary visual cortex, as well as the arrival and synapse formation of geniculate axons within layer IV occurs around P21 in the ferret (Johnson and Casagrande 1993; Jackson et al. 1989), but occurs prenatally in the monkey (Rakic 1977).

Several other aspects of cortical function appear to mature during this same postnatal period shortly after eye opening, over which we observe the major decline in zinc staining in layer IV of areas 17 and 18. (1) While ocular dominance columns are established early in the ferret (P16: Crowley and Katz 2000), the critical period for ocular dominance plasticity roughly coincides with the period of major decline in zinc staining in layer IV and continues until the end of the second postnatal month (Issa et al. 1999). (2) The development and refinement of horizontal projections in layers II/III of ferret visual cortex starts around P22 and continues until distinct adult-like clusters are observed at P45 (Durack and Katz 1996; Ruthazer and Stryker 1996); the refinement of this aspect of cortical circuitry appears adult-like just when zinc staining in the superficial layers of ferret visual cortex first appears adult-like. (3) Chapman and Stryker (1993) showed that orientation selective responses are first detected as early as P23, with 25 % of cells in all layers showing some orientation selectivity. These immature responses continue unchanged until roughly postnatal week five, when the orientation preference of V1 neurons is qualitatively adultlike. (4) Li et al. (2006) used optical imaging and electrophysiological techniques to show that direction selectivity in ferret visual cortex emerges shortly after eye opening, and is qualitatively adultlike by P45. (5) Cortical feedback projections to ferret primary visual cortex also appear to refine to their adultlike state during the second postnatal month (Khalil and Levitt 2008).

The changes in synaptic zinc density we observe during the postnatal development of juvenile ferret visual cortex are consistent with previous studies in other species; cat primary visual cortex (Dyck et al. 1993), rat forebrain (Valente et al. 2002) as well as mouse somatosensory cortex (Czupryn and Skangiel-Kramska 1997; Ichinohe et al. 2006; Land and Shamalla-Hannah 2002). Synaptic zinc has been associated with various forms of experience dependent and developmentally regulated synaptic plasticity. In the rat somatosensory cortex, postnatal reduction in zinc staining is observed in the core of barrels, but high levels can be sustained by depriving the animal of sensory information through whisker trimming (Czupryn and Skangiel-Kramska 2003; Land and Shamalla-Hannah 2002). Furthermore, manipulating sensory experience in adults through whisker trimming causes a rapid and transient elevation of zinc in the core of the barrels (Brown and Dyck 2002, 2005a; Land and Akhtar 1999). Similar effects have been observed in the visual system of the monkey; monocular deprivation provokes a rapid elevation of zinc levels in the deprived eye ocular dominance bands (Dyck and Chaudhuri 2003). An important unanswered question is the role of neurons that use zinc in the maturation, organization, and function of the cerebral cortex. In addition, it is of great interest to reveal if synaptic zinc is simply an indicator of the maturity of a region, or plays a key role in mediating the maturation process.

Asynchronous versus concurrent refinement of zinc-positive circuits in different cortical areas

While some aspects of cortical circuitry may refine concurrently in a number of areas, other aspects exhibit a hierarchical sequence of maturation with primary areas maturing before secondary and multisensory areas. Rakic et al. (1986) provided evidence in support of the concurrent maturation view. They showed that the rapid proliferation phase of cortical synaptogenesis and subsequent refinement occurs simultaneously in multiple and diverse regions of the cerebral cortex. In contrast, Condé et al. (1996) suggested asynchronous postnatal maturation of macaque cortical areas by showing that a subclass of local circuit neurons are adult-like first in primary sensory areas, but later in higher-order association areas. Bourne and Rosa (2006) provided more evidence in support of the concept of hierarchical maturation of cortical areas by noting that a subset of pyramidal neurons in V1, MT, S1, and A1 were histochemically mature at birth in New World monkeys, but not in higher-order association areas.

We have demonstrated reorganization of zinc circuits in ferret visual cortex during the second postnatal month, the period immediately after eye opening. Most strikingly, the reduction in zinc density is greater in layer IV of areas 17 and 18 than in areas 19, 21, and Ssy. One could argue that our results reveal different rates of zinc circuit refinement in different areas as the rate and magnitude of change differs between areas 17 and 18 versus areas 19, 21, and Ssy. This presumably reflects changes in the relative weight of thalamocortical versus corticocortical inputs to those areas. However, although areas 17 and 18 show a greater decline in zinc staining than areas 19, 21, and Ssy, minimum staining intensity in all areas is reached at the same postnatal age (6 weeks), and therefore developmental trajectories among areas appear fundamentally similar in this respect. In contrast, another indicator of glutamatergic system maturation appears clearly asynchronous; different vesicular glutamate transporters (VGLuT1) and (VGLuT2), which are differentially expressed in particular brain circuits, have been shown to refine on different time scales (Liguz-Lecznar and Skangiel-Kramska 2007; Nakamura et al. 2005). Whether areas 17 and 18 share a different developmental timecourse for zinc staining than areas 19, 21, and Ssy, or all areas manifest a similar rate of change is open to interpretation.

Acknowledgments

Supported by grants from the NSF (0619290), National Center for Research Resources (2G12RR03060-26A1) and the National Institute on Minority Health and Health Disparities (8G12MD007603-27) from the National Institutes of Health, and Professional Staff Congress-City University of New York (PSC-CUNY). The authors thank Vidyasagar Sriramoju for suggesting the use of zinc histochemistry.

References

Barnette AR, Neil JJ, Kroenke CD, Griffith JL, Epstein AA, Bayly PV, Knutsen AK, Inder TE. Characterization of brain development in the ferret via MRI. Pediatr Res. 2009; 66(1):80–84. [PubMed: 19287340]

Beaulieu C, Dyck R, Cynader M. Enrichment of glutamate in zinc-containing terminals of the cat visual cortex. NeuroReport. 1992; 3(10):861–864. [PubMed: 1358251]

Bourne JA, Rosa MG. Hierarchical development of the primate visual cortex, as revealed by neurofilament immunoreactivity: early maturation of the middle temporal area (MT). Cereb Cortex. 2006; 3:405–414. [PubMed: 15944371]

Brown CE, Dyck RH. Rapid, experience-dependent changes in levels of synaptic zinc in primary somatosensory cortex of the adult mouse. J Neurosci. 2002; 22(7):2617–2625. [PubMed: 11923427]

Brown CE, Dyck RH. Distribution of zincergic neurons in the mouse forebrain. J Comp Neurol. 2004; 479(2):156–167. [PubMed: 15452827]

Brown CE, Dyck RH. Modulation of synaptic zinc in barrel cortex by whisker stimulation. Neuroscience. 2005a; 134(2):355–359. [PubMed: 16019150]

Brown CE, Dyck RH. Retrograde tracing of the subset of afferent connections in mouse barrel cortex provided by zincergic neurons. J Comp Neurol. 2005b; 486(1):48–60. [PubMed: 15834958]

Cantone G, Xiao J, McFarlane N, Levitt JB. Feedback connections to ferret striate cortex: direct evidence for visuotopic convergence of feedback inputs. J Comp Neurol. 2005; 487:312–331. [PubMed: 15892103]

Casanovas-Aguilar C, Miro-Bernie N. Zinc-rich neurones in the rat visual cortex give rise to two laminar segregated systems of connections. Neuroscience. 2002; 110(3):445–458. [PubMed: 11906785]

Casanovas-Aguilar C, Reblet C, Perez-Clausell J, Bueno-Lopez JL. Zinc-rich afferents to the rat neocortex: projections to the visual cortex traced with intracerebral selenite injections. J Chem Neuroanat. 1998; 15(2):97–109. [PubMed: 9719362]

Casanovas-Aguilar C, Christensen MK, Reblet C, Martinez-Garcia F, Pérez-Clausell J, Bueno-Lopez JL. Callosal neurones give rise to zinc-rich boutons in the rat visual cortex. NeuroReport. 1995; 6:497–500. [PubMed: 7539303]

Chapman B, Stryker MP. Development of orientation selectivity in ferret visual cortex and effects of deprivation. J Neurosci. 1993; 13(12):5251–5262. [PubMed: 8254372]

Clancy B, Darlington RB, Finlay BL. Translating developmental time across mammalian species. J Neurosci. 2001; 105(1):7–17.

Condé F, Lund JS, Lewis DA. The hierarchical development of monkey visual cortical regions as revealed by the maturation of parvalbumin-immunoreactive neurons. Brain Res Dev Brain Res. 1996; 96(1–2):261–276.

Crowley JC, Katz LC. Early development of ocular dominance columns. Science. 2000; 290(5495): 1321–1324. [PubMed: 11082053]

Czupryn A, Skangiel-Kramska J. Distribution of synaptic zinc in the developing mouse somatosensory barrel cortex. JCN. 1997; 386:652–660.

Czupryn A, Skangiel-Kramska J. Switch time-point for rapid experience-dependent changes in zinc-containing circuits in the mouse barrel cortex. Brain Res Bull. 2003; 61(4):385–391. [PubMed: 12909281]

Danscher G. Exogenous selenium in the brain: a histochemical technique for light and electron microscopic localization of catalytic selenium bonds. Histochemistry. 1982; 76:4281–4293.

Danscher G, Howell G, Pérez-Clausell J, Hertel N. The dithizone, Timm's sulphide silver and the selenium methods demonstrate a chelatable pool of zinc in CNS: a proton activation (PIXE) analysis of carbon tetrachloride extracts from rat brains and spinal cords intravitall treated with dithizone. Histochem-istry. 1985; 83:419–422.

Durack JC, Katz LC. Development of horizontal projections in layer 2/3 of ferret visual cortex. Cereb Cortex. 1996; 6(2):178–183. [PubMed: 8670648]

Dyck RH, Chaudhuri A. Experience-dependent regulation of the zincergic innervation of visual cortex in adult monkeys. Cereb Cortex. 2003; 13(10):1094–1109. [PubMed: 12967926]

Dyck R, Beaulieu C, Cynader M. Histochemical localization of synaptic zinc in the developing cat visual cortex. J Comp Neurol. 1993; 329(1):53–67. [PubMed: 8384221]

Finney EM, Stone JR, Shatz CJ. Major glutamatergic projection from subplate into visual cortex during development. J Comp Neurol. 1998; 398(1):105–118. [PubMed: 9703030]

Frederickson CJ. Neurobiology of zinc and zinc-containing neurons. Int Rev Neurobiol. 1989; 31:145–238. [PubMed: 2689380]

Frederickson CJ. Imaging zinc: old and new tools. Sci STKE. 2003; 182:pe18. [PubMed: 12746547]

Frederickson, CJ.; Danscher, G. Hippocampal zinc, the storage granule pool: localization, physiochemistry, and possible functions. In: Morley, JE.; Sterman, MB.; Walsh, JH., editors. Nutritional modulation of neural function. Academic Press; San Diego: 1988. p. 289-306.

Frederickson CJ, Rampy BA, Reamy-Rampy S, Howell GA. Distribution of histochemically reactive zinc in the forebrain of the rat. J Chem Neuroanat. 1992; 5:521–530. [PubMed: 1476668]

Friauf E, McConnell SK, Shatz CJ. Functional synaptic circuits in the subplate during fetal and early postnatal development of cat visual cortex. J Neurosci. 1990; 10:2601–2613. [PubMed: 2388080]

Gallyas F. Silver staining of myelin by means of physical development. Neurol Res. 1979; 1(2):203–209. [PubMed: 95356]

Garrett B, Slomianka L. Postnatal development of zinc-containing cells and neuropil in the visual cortex of the mouse. Anat Embryol (Berl). 1992; 186(5):487–496. [PubMed: 1443656]

Garrett B, Geneser FA, Slomianka L. Distribution of acetyl-cholinesterase and zinc in the visual cortex of the mouse. Anat Embryol (Berl). 1991; 184(5):461–468. [PubMed: 1741478]

Garrett B, Sørensen JC, Slomianka L. Fluoro-gold tracing of zinc-containing afferent connections in the mouse visual cortices. Anat Embryol (Berl). 1992; 185(5):451–459. [PubMed: 1567021]

Garrett B, Osterballe R, Slomianka L, Geneser FA. Cytoar-chitecture and staining for acetylcholinesterase and zinc in the visual cortex of the Parma wallaby (Macropus parma). Brain Behav Evol. 1994; 43(3):162–172. [PubMed: 8193908]

Ghosh A, Shatz CJ. Involvement of subplate neurons in the formation of ocular dominance columns. Science. 1992; 255:1441–1443. [PubMed: 1542795]

Homman-Ludiye J, Manger PR, Bourne JA. Immunohisto-chemical parcellation of the ferret (*Mustela putorius*) visual cortex reveals substantial homology with the cat (*Felis catus*). J Comp Neurol. 2010; 518(21):4439–4462. [PubMed: 20853515]

Ichinohe N, Potapov D, Rockland KS. Transient synaptic zinc-positive thalamocortical terminals in the developing barrel cortex. Eur J Neurosci. 2006; 24(4):1001–1010. [PubMed: 16930427]

Ichinohe N, Matsushita A, Ohta K, Rockland KS. Pathway-specific utilization of synaptic zinc in the macaque ventral visual cortical areas. Cereb Cortex. 2010; 20:2818–2831. [PubMed: 20211942]

Innocenti GM, Manger PR, Masiello I, Colin I, Tettoni L. Architecture and callosal connections of visual areas 17, 18, 19 and 21 in the ferret (*Mustela putorius*). Cereb Cortex. 2002; 12(4):411–422. [PubMed: 11884356]

Issa NP, Trachtenberg JT, Chapman B, Zahs KR, Stryker MP. The critical period for ocular dominance plasticity in the ferret's visual cortex. J Neurosci. 1999; 19(16):6965–6978. [PubMed: 10436053]

Jackson CA, Peduzzi JD, Hickey TL. Visual cortex development in the ferret. I. Genesis and migration of visual cortical neurons. J Neurosci. 1989; 9:1242–1253. [PubMed: 2703875]

Johnson JK, Casagrande VA. Prenatal development of axon outgrowth and connectivity in the ferret visual system. Vis Neurosci. 1993; 10:117–130. [PubMed: 8424921]

Kaas, JH. Cortical areas, unity and diversity. CRC press; Boca Raton: 2002. Cortical areas and patterns of cortico-cortical connections; p. 179-191.

Khalil, R.; Levitt, JB. Society for Neuro-science Abstracts. 2008. Postnatal refinement of cortical feedback connections to ferret primary visual cortex.

Kanold PO, Kara P, Reid RC, Shatz CJ. Role of subplate neurons in functional maturation of visual cortical columns. Science. 2003; 301(5632):521–525. [PubMed: 12881571]

Land PW, Akhtar ND. Experience-dependent alteration of synaptic zinc in rat somatosensory barrel cortex. Somatosens Mot Res. 1999; 16(2):139–150. [PubMed: 10449062]

Land PW, Shamalla-Hannah L. Experience-dependent plasticity of zinc-containing cortical circuits during a critical period of postnatal development. J Comp Neurol. 2002; 447(1):43–56. [PubMed: 11967894]

Li Y, Fitzpatrick D, White LE. The development of direction selectivity in ferret visual cortex requires early visual experience. Nat Neurosci. 2006; 9(5):676–681. [PubMed: 16604068]

Liguz-Lecznar M, Skangiel-Kramska J. Vesicular glutamate transporters VGLUT1 and VGLUT2 in the developing mouse barrel cortex. Int J Dev Neurosci. 2007; 25(2):107–114. [PubMed: 17289331]

Martinez-Guijarro FJ, Soriano E, Del Rio JA, Lopez-Garcia C. Zinc-positive boutons in the cerebral cortex of lizards show glutamate immunoreactivity. J Neurocytol. 1991; 20(10):834–843. [PubMed: 1723751]

McConnell SK, Ghosh A, Shatz CJ. Subplate neurons pioneer the first axon pathway from the cerebral cortex. Science. 1989; 245:978–982. [PubMed: 2475909]

Molnar Z, Adams R, Blakemore C. Mechanisms underlying the early establishment of thalamocortical connections in the rat. J Neurosci. 1998; 18:5723–5745. [PubMed: 9671663]

Nakamura K, Hioki H, Fujiyama F, Kaneko T. Postnatal changes of vesicular glutamate transporter (VGluT)1 and VGluT2 immunoreactivities and their colocalization in the mouse forebrain. J Comp Neurol. 2005; 492(3):263–288. [PubMed: 16217795]

Nakashima A, Dyck RH. Zinc and cortical plasticity. Brain Res Rev. 2009; 59:347–373. [PubMed: 19026685]

Pérez-Clausell J. Distribution of terminal fields stained for zinc in the neocortex of the rat. J Chem Neuroanat. 1996; 11(2):99–111. [PubMed: 8877598]

Rakic P. Prenatal development of the visual system in rhesus monkey. Phil Trans R Soc Lond B. 1977; 278(961):245–260. [PubMed: 19781]

Rakic P, Bourgeois JP, Eckenhoff MF, Zecevic N, Goldman-Rakic PS. Concurrent overproduction of synapses in diverse regions of the primate cerebral cortex. Science. 1986; 232(4747):232–235. [PubMed: 3952506]

Rockland KS, Pandya DN. Laminar origins and terminations of cortical connections of the occipital lobe in the rhesus monkey. Brain Res. 1979; 179(1):3–20. [PubMed: 116716]

Ruthazer ES, Stryker MP. The role of activity in the development of long-range horizontal connections in area 17 of the ferret. J Neurosci. 1996; 16(22):7253–7269. [PubMed: 8929433]

Valente T, Auladell C, Pérez-Clausell J. Postnatal development of zinc-rich terminal fields in the brain of the rat. Exp Neurol. 2002; 174(2):215–229. [PubMed: 11922663]

Wong-Riley M. Changes in the visual system of monocularly sutured or enucleated cats demonstrable with cytochrome oxidase histochemistry. Brain Res. 1979; 171(1):11–28. [PubMed: 223730]

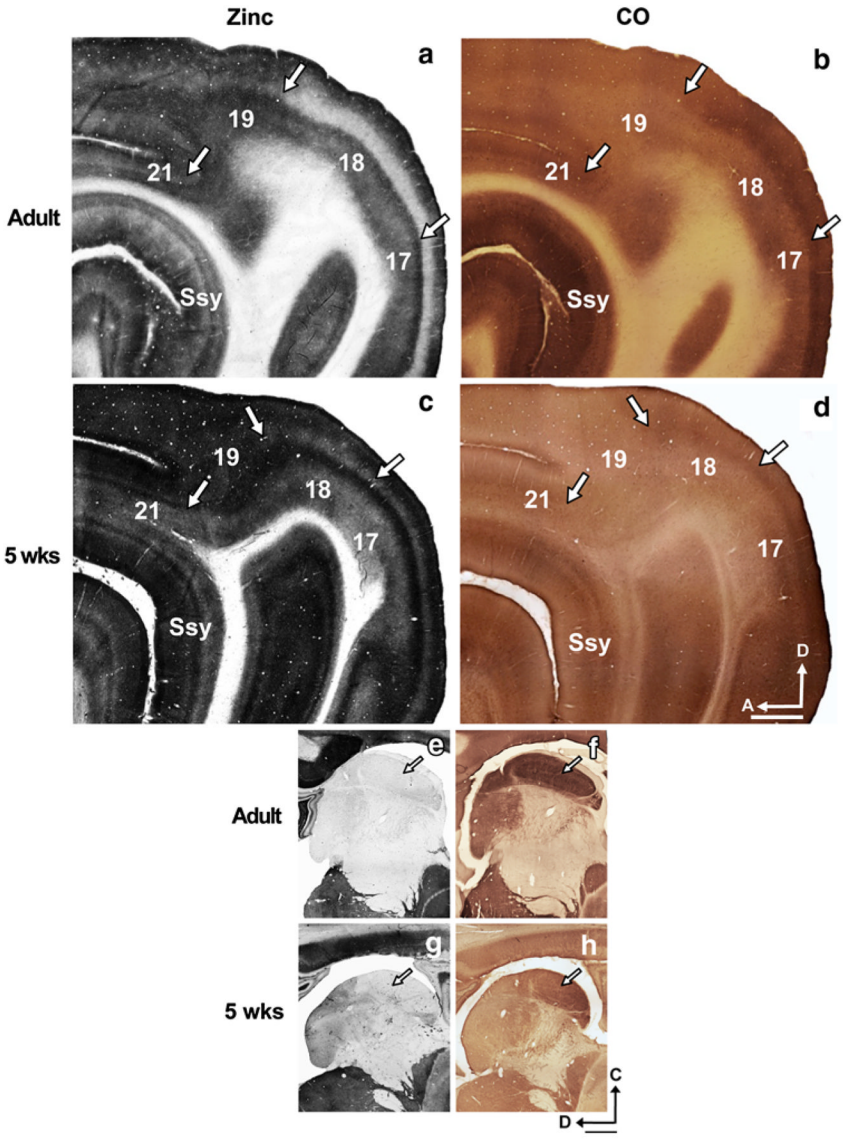

Fig. 1.

Synaptic zinc staining in the adult and juvenile ferret brain distinguishes different visual cortical areas. Photomicrographs of adjacent semi-tangential sections stained for **a** synaptic zinc or **b** cytochrome oxidase (CO) in the adult, and **c** synaptic zinc or **d** CO in the 5-week-old juvenile. *Arrows* mark areal boundaries. Photomicrographs of adjacent semi-tangential sections of thalamus stained for **e** synaptic zinc or **f** CO in the adult, and **g** synaptic zinc or **h** CO in the 5-week-old juvenile. Arrows indicate lateral geniculate nucleus. *Ssy* Suprasylvian cortex, *A* anterior, *D* dorsal. *Scale bar* 1 mm

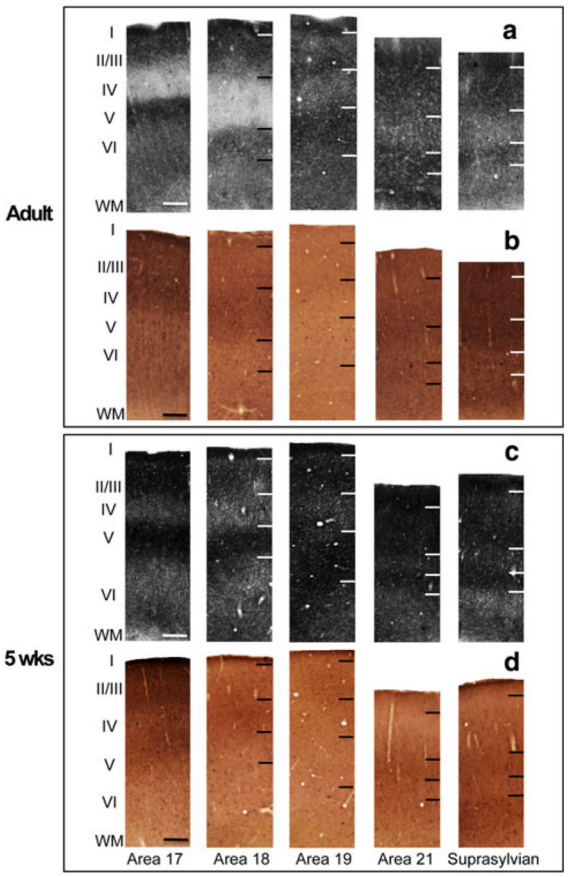

Fig. 2.

Laminar variation of zinc and CO staining in different visual cortical areas in the adult and juvenile ferret. Photomicrographs of columns taken from adjacent sections in adult cortex stained for **a** synaptic zinc or **b** CO, and juvenile cortex stained for **c** synaptic zinc or **d** CO. *roman numerals* indicate cortical layers (I–VI). *Scale bar* 200 μm

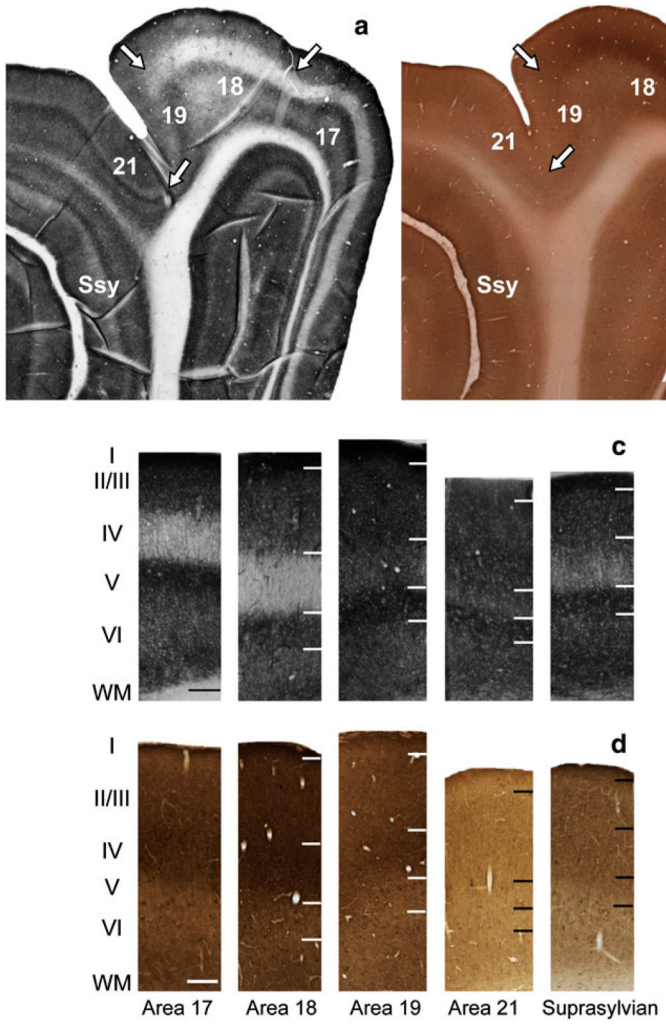

Fig. 3.

Synaptic zinc staining and laminar variation in the 9-week-old juvenile ferret brain distinguishes different visual cortical areas.

Photomicrographs of adjacent semi-tangential sections stained for **a** synaptic zinc or **b** (CO). Photomicrographs of columns taken from adjacent sections stained for **c** synaptic zinc or **d** CO. *Ssy* Suprasylvian cortex, *A* anterior, *D* dorsal. *Scale bar* 1 mm

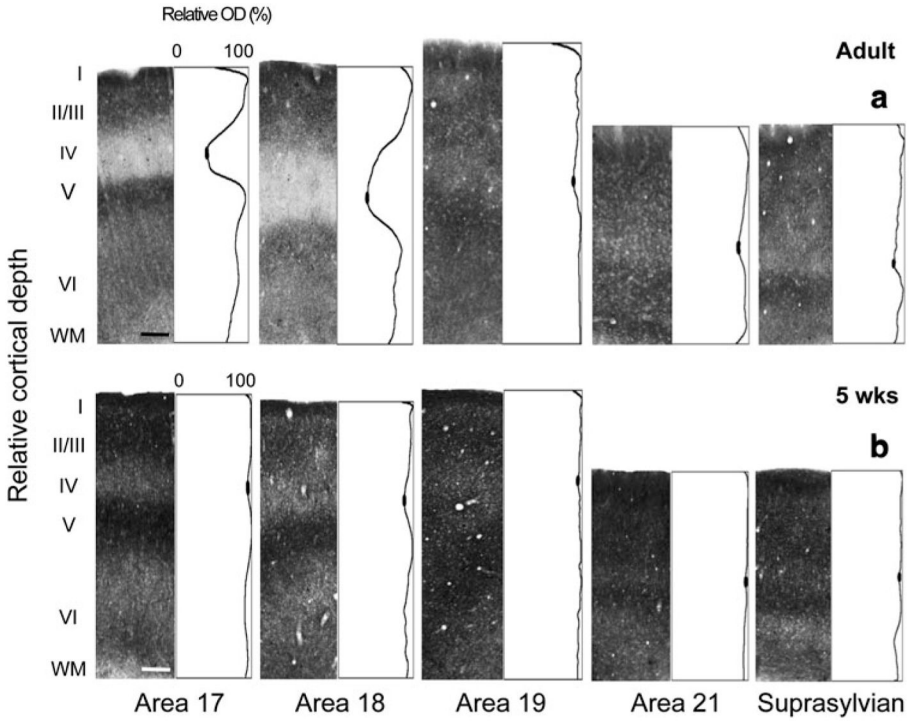

Fig. 4.

Laminar distribution of synaptic zinc in different visual cortical areas in the adult and juvenile ferret. Representative photomicrographs of columns through all cortical layers with corresponding normalized optical density profiles in **a** adult and **b** 5-week-old. Low synaptic zinc density in layer IV of adult areas 17 and 18 is indicated by the trough in the profile plot. In each plot profile, *filled ovals* in the trough of layer IV indicate the values used to determine average minimum pixel intensity value. *Scale bar* 200 μm

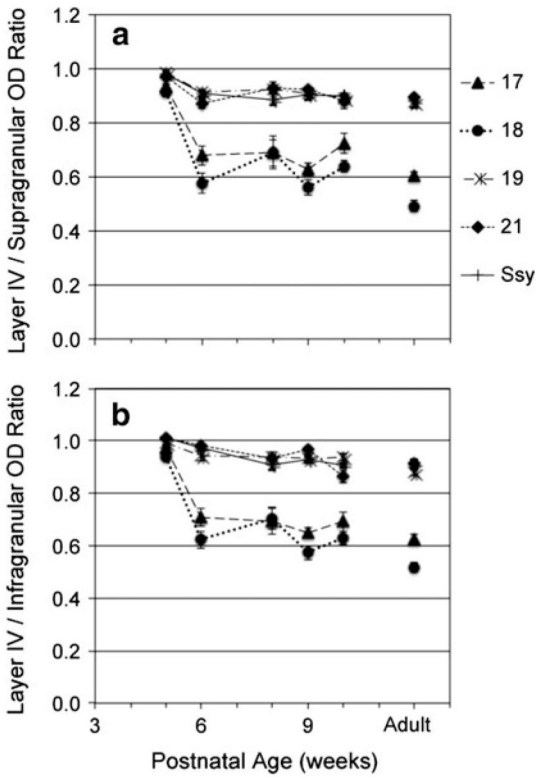

Fig. 5.

Ratio of synaptic zinc optical density in layer IV relative to that in the supragranular (**a**) and infragranular (**b**) layers in different visual cortical areas at different postnatal ages. Adult mean values are plotted on the *right* for comparison. *Error bars* represent ±SEM

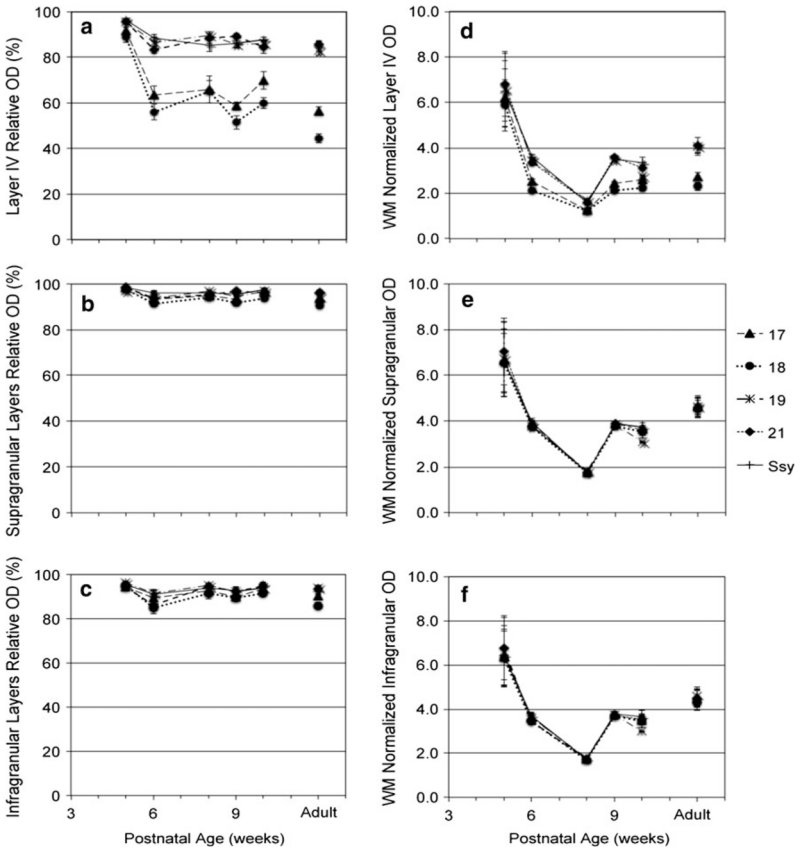

Fig. 6.

Average normalized synaptic zinc optical density (OD) in layer IV, supragranular II/III, and infragranular V/VI (**a–c**), and average white matter (WM) normalized synaptic zinc (OD) in layer IV, supragranular II/III, and infragranular V/VI (**d–f**) in different visual cortical areas at different postnatal ages. Adult mean values are plotted on the *right* for comparison. *Error bars* represent ±SEM